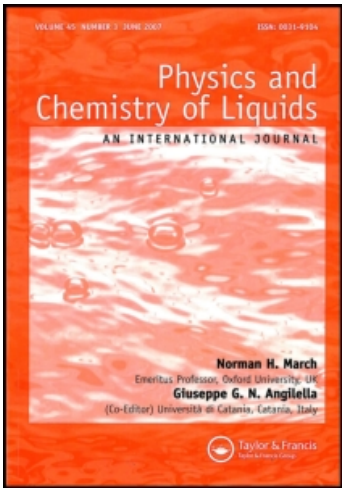

Physics and Chemistry of Liquids
Publication details, including instructions for authors and subscription information:
http://www.informaworld.com/smpp/title~content=t713646857

Re-entrant melting of the exp-6 fluid: the role of the repulsion softness

Franz Saija[a]; Gianpietro Malescio[b]; Santi Prestipino[b]
[a] CNR-Istituto per i Processi Chimico-Fisici, 98158 Messina, Italy [b] Dipartimento di Fisica, Università degli Studi di Messina, 98166 Messina, Italy

Online publication date: 14 July 2010

To cite this Article Saija, Franz , Malescio, Gianpietro and Prestipino, Santi(2010) 'Re-entrant melting of the exp-6 fluid: the role of the repulsion softness', Physics and Chemistry of Liquids, 48: 4, 477 — 487
To link to this Article: DOI: 10.1080/00319100903131542
URL: http://dx.doi.org/10.1080/00319100903131542

Physics and Chemistry of Liquids
Vol. 48, No. 4, August 2010, 477–487

Taylor & Francis
Taylor & Francis Group

Re-entrant melting of the exp-6 fluid: the role of the repulsion softness

Franz Saija[a]*, Gianpietro Malescio[b] and Santi Prestipino[b]

[a]*CNR-Istituto per i Processi Chimico-Fisici, Contrada Papardo, 98158 Messina, Italy;*
[b]*Dipartimento di Fisica, Università degli Studi di Messina, Contrada Papardo, 98166 Messina, Italy*

(*Received 5 June 2009; final version received 20 June 2009*)

We investigate the phase behaviour of a system of particles interacting through the exp-6 pair potential, an interaction model that is appropriate to describe effective interatomic forces under high compression. The soft-repulsive component of the potential is being varied so as to study the effect on re-entrant melting and density anomaly. Upon increasing the repulsion softness, we find that the anomalous melting features persist and occur at lower pressures. Moreover, if we reduce the range of downward concavity in the potential by extending the hard core at the expenses of the soft-repulsive shoulder, the re-entrant part of the melting line reduces in extent so as it does the region of density anomaly.

Keywords: high-pressure phase diagram; liquid–solid transitions; re-entrant melting

1. Introduction

At high pressures, a number of elements in the periodic table show a maximum in the fluid–solid coexistence temperature, followed by a region of re-entrant melting, see, e.g. Cs, Rb, Na, Ba, Te, etc. [1]. A further pressure increase makes the slope of the melting line positive again. This behaviour has been called 'anomalous', as opposed to the 'standard' behaviour typical of simple fluids, consisting in a regularly increasing and concave melting curve. The class of substances exhibiting anomalous melting constantly expands as advances in experimental methods allow to reach higher pressures. Anomalous melting has been related to a certain degree of softness, as induced by pressurization, of the interatomic repulsion [2–5]. A similar behaviour is observed in a completely different type of systems, i.e. polymer solutions and colloidal dispersions [6–9], where it usually appears in combination with other water-like anomalies [10,11]. In order to account for these melting oddities, numerous effective pair potentials were proposed in the past, some of them being even bounded at zero separation [2,12–19]. Core-softened potentials generally present a region of downward concavity in their repulsive component [20].

A classical spherically-symmetric potential that is widely used in the realm of high-pressure physics is the Buckingham, or exp-6 potential [4,21], where the short-range

*Corresponding author. Email: saija@me.cnr.it

ISSN 0031–9104 print/ISSN 1029–0451 online

DOI: 10.1080/00319100903131542
http://www.informaworld.com

repulsion is modelled through a hard-core plus a soft-repulsive exponential shoulder:

$$u(r) = \begin{cases} +\infty, & r < \sigma_M \\ \frac{\epsilon}{\alpha-6}\left[6e^{-\alpha(r/\sigma-1)} - \alpha\left(\frac{\sigma}{r}\right)^6\right], & r \geq \sigma_M \end{cases}. \quad (1)$$

Here r is the interparticle distance, ϵ is the depth of the attractive well, σ is the position of the well minimum, α (usually taken in the range 10–15 [22]) controls the steepness of the exponential repulsion, and $\sigma_M(\alpha)$ is the point where the function in the second line of Equation (1) attains its maximum value. The exp-6 potential satisfies the core-softening condition, i.e. there exists a range of interparticle distances where the repulsive force decreases as two particles get closer to each other [23]. This gives origin to two separate repulsive length scales, i.e. a larger one associated with the soft repulsion (being effective at the lower pressures) and a smaller one related to the particle-core diameter σ_M (dominant at higher pressures). It has been shown that, upon increasing the pressure P, the melting temperature of the exp-6 system passes through a maximum followed by a region of re-entrant melting; upon further compression, the melting line eventually recovers a positive slope [23]. This behaviour is related to the existence of two different patterns of short-range order in the system: an open one (associated with the soft-repulsive scale) and a compact one (associated with the hard core). The re-entrance of the fluid phase at intermediate pressures (and for not too low temperatures) follows from the packing frustration induced by the interplay between these two local structures.

To better understand the role of the soft repulsion for the occurrence of anomalous melting, we investigate how the phase behaviour of the exp-6 model changes when varying the softness of the potential. This variation can be achieved in two ways. The most direct one is by changing the exponent α controlling the steepness of the exponential repulsion. A different way of varying the degree of softness is to define, for fixed α, a whole sequence of modified exp-6 interactions by shifting to higher distance, the point where the repulsion changes from hard-core to exponential. For the original exp-6 interaction, this crossing point occurs at $r_{\text{cross}} = \sigma_M$; taking r_{cross} to be larger than σ_M, the ensuing repulsion turns out to be softer than the exp-6 law.

This article is organised as follows: in Section 2, we introduce the numerical approach that is used to construct the phase diagram of the system; Section 3 is devoted to a discussion of the results while further remarks and conclusions are deferred to Section 4.

2. Monte Carlo simulation

We perform Monte Carlo (MC) simulations of the exp-6 model in the isothermal–isobaric (NPT) ensemble, where N is the number of particles, P is the pressure and T is the temperature, using the standard Metropolis algorithm and periodic boundary conditions. The simulations are carried out for a number $N = 432$ (bcc) and $N = 500$ particles (fcc) in a cubic box (we checked that finite-size effects are negligible). For each pressure P and temperature T, equilibration of the sample typically takes some 10^4 MC sweeps, a sweep consisting of N attempts to change the position of a random particle, followed by one attempt to modify the box volume.

The maximum random displacement of a particle and the maximum volume update in a trial MC move are adjusted for every sweep during the run so as to keep the acceptance ratio of the moves as close to 50% as possible, with only small excursions around this value. For given *NPT* conditions, the relevant thermodynamic averages are computed over a trajectory of length ranging from 5×10^4 to 10^5 sweeps.

In order to locate the melting line, we generate a series of isobaric paths starting, at very low T, from perfect crystals, which are then heated gradually until melting occurs. This is evidenced by the abrupt change in, e.g. the energy (Figure 1) as well as by the rounding off of the peaks of the radial distribution function (RDF). In fact, by this so-called 'heat-until-it-melts' (HUIM) approach only the temperature T^+ of maximum solid overheating is calculated, which might be considerably larger than the melting temperature T_m [24]. Similarly, the maximum fluid supercooling temperature T^- is generally far from T_m, in fact, farther than T^+. For a Lennard–Jones system, Luo et al. [24] found that the extent of maximum overheating/supercooling is only weakly pressure-dependent; moreover, they suggest the empirical formula $T_m = T^+ + T^- - \sqrt{T^+T^-}$ for extracting T_m from the boundaries of the hysteresis loop. Another

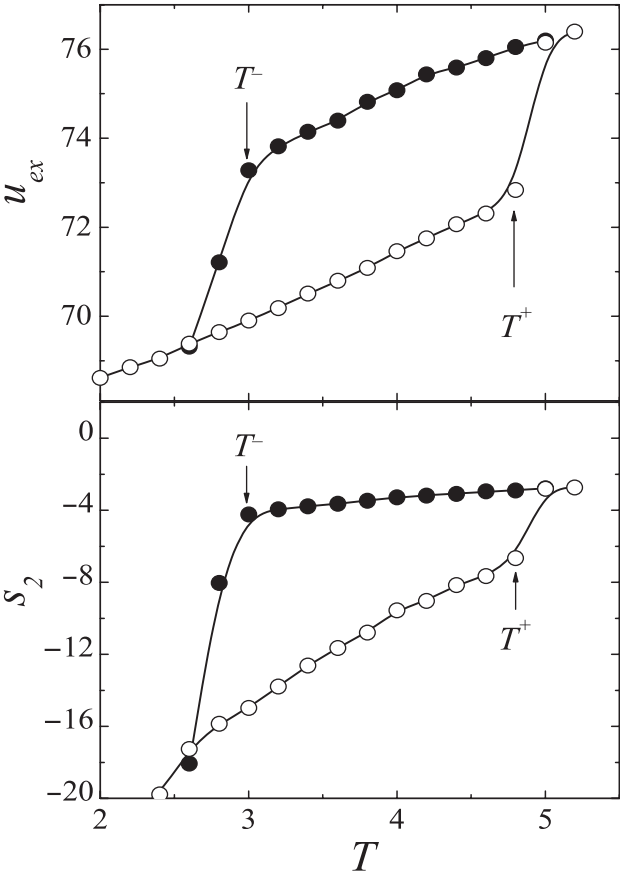

Figure 1. Modified exp-6 potential with $r_{\text{cross}} = 0.5$ at $P = 1000$: the bcc-fluid hysteresis loop for the excess energy (top panel) and the two-body entropy [24] (bottom panel) at $P = 1000$. Pressure P and temperature T and expressed in units of ϵ/σ^3 and ϵ/K_B, respectively.

possibility, which we prefer because it does not rely on a specific system, is to appeal to the Landau theory of weak first-order transitions [25], which gives the relation $T_m = (T^- + 8T^+)/9$. In all cases here examined, we have verified that the deviation of T^+ from the Landau-type estimate of T_m is small (6% at the most) and almost insensitive to pressure. This indicates that the overall shape of the coexistence curve, which we are more interested in, is correctly got by the simple HUIM method.

In addition, we calculate the pair excess entropy for each state point:

$$s_2 = -\frac{k_B}{2}\rho \int d\mathbf{r}[\, g(r)\ln g(r) - g(r) + 1], \tag{2}$$

where k_B is Boltzmann's constant, ρ is the number density, and $g(r)$ is the RDF. $-s_2$ effectively characterises the degree of pair translational order in the fluid, as such providing a good indicator of the melting transition, much better than the density which has a larger noise-to-signal ratio (Figure 1, bottom panel) [26].

An independent estimate of the location of the melting line is obtained by the Lindemann criterion [27,28]. The Lindemann ratio, L, is defined as the mean root square displacement of the particles about their equilibrium lattice positions, divided by the nearest-neighbour distance a:

$$L = \frac{1}{a}\left\langle \frac{1}{N}\sum_{i=1}^{N}(\Delta\mathbf{R}_i)^2 \right\rangle^{1/2}, \tag{3}$$

where the brackets $\langle \cdots \rangle$ denote an average over the MC trajectory. The Lindemann rule states that the crystal melts when L becomes larger than some threshold value L_c, which is known to be 0.15–0.16 for a fcc solid and 0.18–0.19 for a bcc solid [29,30]. As we shall see below, the results obtained by the HUIM approach and by the Lindemann rule compare fairly well with each other.

3. Results and discussion

We first computed the exp-6 phase diagram for $\alpha = 10$ (Figure 2). As anticipated, we approximate the melting temperature T_m with the temperature T^+ of maximum solid overheating, assuming that the difference between the two is indeed minute in relative terms and almost the same at all pressures. By comparing the phase diagram of Figure 2 with that for $\alpha = 11$, reported in [23], we observe that the overall shape of the melting line is similar, with the fluid–solid coexistence line passing through a maximum at temperature T_M and pressure P_M. When increasing pressure at a sufficiently low temperature $T < T_M$, the initial fluid system becomes denser and denser until it crystallises into a fcc solid. Upon increasing P further, the fcc solid undergoes a transition to a bcc solid. This transition is related to a decrease in the mean nearest-neighbour distance with increasing pressure, which brings particles to experience inner regions of the interaction potential where the repulsion becomes softer. As the pressure further increases, the bcc solid undergoes re-entrant melting into a denser fluid. At very high pressures, far beyond the region shown in Figure 2, the fluid eventually crystallises into a fcc hard-sphere-like solid. In the fluid region above the re-entrant melting line, decreasing temperature at constant pressure leads first to system compression, and then, contrary to standard behaviour, to an

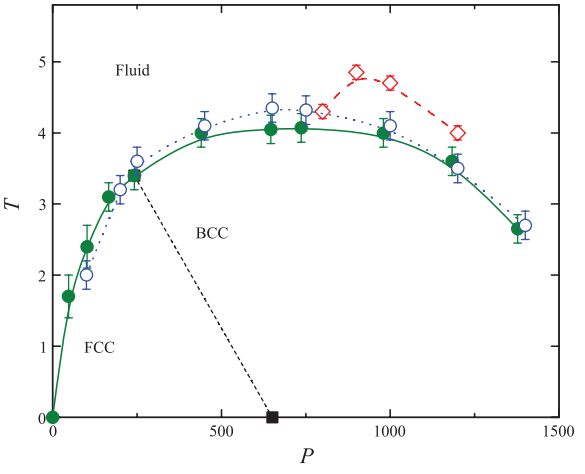

Figure 2. (Colour online). Phase diagram of the exp-6 model for $\alpha = 10$. Pressure P and temperature T are expressed in units of ϵ/σ^3 and ϵ/k_B, respectively. Melting points, located by the Lindemann criterion, are represented as full green dots. The boundary between the bcc and fcc solids (black dotted line) is roughly obtained by drawing a straight line from the full square at $T = 0$ (obtained through an exact total-energy calculation) to the square, lying on the melting curve, where the value of the Lindemann ratio switches from 0.15–0.16 (fcc) to 0.18–0.19 (bcc) [29,30]. We also plot the fluid–solid coexistence locus as obtained by the HUIM criterion (blue open dots), which indeed agrees well with the Lindemann-based estimate. The locus of density maxima in the fluid phase is marked by red diamonds. All lines in the figure are guides to the eye.

expansion for further cooling (Figure 3). The locus of points where the density attains its maximum value encloses a region where the density behaves anomalously (Figure 2). Within this region, open local structures are more favoured than compact ones, causing a diminution of the number of particles within a given volume with decreasing T. A similar density anomaly has been observed in a number of substances (water being the most familiar) as well as in model systems characterised by a soft repulsion [19,31–33].

We computed the RDF at a temperature slightly larger than T_M, in the pressure range where re-entrant melting occurs (Figure 4). At low pressure, the soft repulsion is quite effective and particles cannot stay too close to each other. Upon increasing pressure at constant temperature, more and more particles are able to overcome the soft repulsion, thus giving origin to a peak close to the hard core whose height increases with pressure. Meanwhile the second and third peak become lower, reflecting the loss of efficacy of the soft-repulsive length scale. Thus, an increase of pressure causes the gradual turning off of the soft-repulsive length scale in favour of the smaller length scale associated with the inner core. The observed behaviour differs significantly from that of simple fluids, where all the peaks of $g(r)$ get higher as pressure grows at constant T.

We now follow a different approach for varying the softness of the exp-6 potential, one in which the parameter α is left unchanged. An important feature of the exp-6 potential, with regard to its soft nature, is the existence of a range of interparticle distances where the repulsive force decreases as two particles get closer.

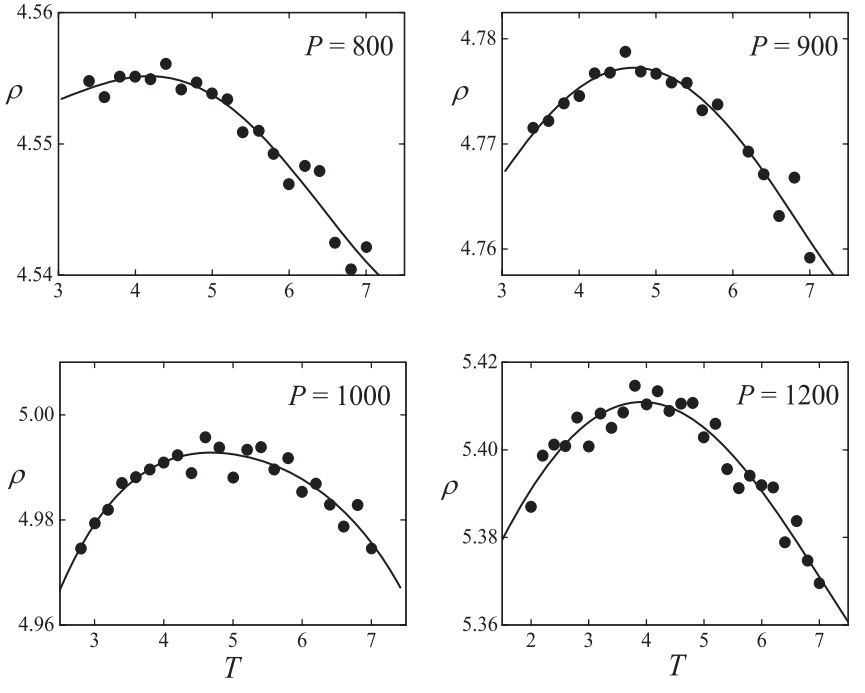

Figure 3. Exp-6 model for $\alpha = 10$: fluid number density ρ(in units of σ^{-3}) as a function of temperature for $P = 800$, 900, 1000, 1200 (full dots). All lines are fourth-order polynomial fits of the data points.

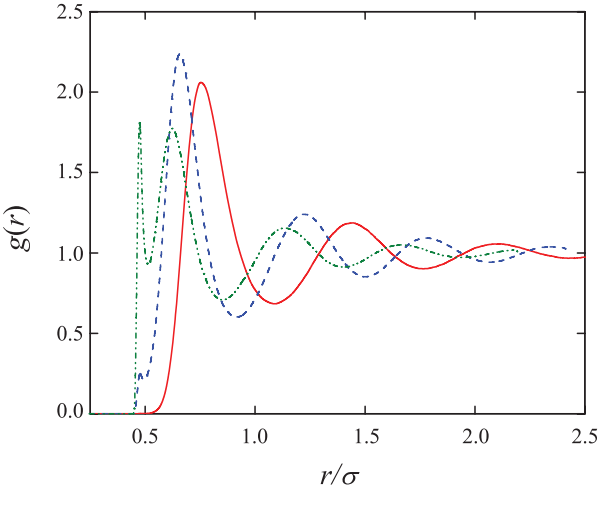

Figure 4. (Colour online). Exp-6 model for $\alpha = 10$: RDF $g(r)$ for $T = 5$ and three pressures, $P = 150$ (red solid line), 750 (blue dashed line), 1500 (green dash-dotted line).

This interval corresponds to the concave part of the potential, which, in the original exp-6 potential, extends from σ_M up to the inflection point σ_F. In the exp-6 model, the value r_{cross} of the interparticle distance where the repulsion changes from hard core to soft is σ_M. Instead, we allow here r_{cross} to increase progressively, thus shrinking the interval where the potential is downward concave, until this interval disappears when r_{cross} reaches σ_F (Figure 5). In this way we are able to vary the relative importance of the hard and soft components of the exp-6 repulsion.

We have calculated the melting line for a number of 'modified' exp-6 potentials with $\alpha = 10$ by the HUIM approach, (Figure 6). For increasing r_{cross}, the portion of the melting curve preceding the maximum (i.e. for $P < P_M$) remains substantially unaltered, while that having negative slope becomes more and more flat until, for a value of r_{cross} slightly smaller than σ_F, the slope dT/dP becomes everywhere positive and the melting-curve maximum disappears. Upon further increasing r_{cross}, the part of the melting line for $P > P_M$ becomes steeper. This behaviour clearly underlines the fundamental role played by the soft-repulsive component of the potential in giving origin to re-entrant melting. We stress that the re-entrant region, in fact, disappears for a value of r_{cross} being a little smaller than σ_F, that is when the potential has still an interval of downward concavity. This suggests that the existence of a concave repulsive region in the potential, while being crucial for re-entrant melting, is not strictly sufficient for its occurrence. This result is consistent with the findings of a recent investigation of the phase behaviour of a potential consisting in a smoothened hard core plus a repulsive step, showing that a melting line with a maximum and a re-entrant portion occurs only for a sufficiently wide repulsive shoulder [34].

As r_{cross} increases, the region of anomalous density behaviour becomes less evident until it disappears completely, at least in the stable fluid phase, when the slope dT/dP becomes everywhere positive (Figure 7). Actually, with increasing r_{cross}, the density anomaly migrates to lower temperatures, while the melting line moves to

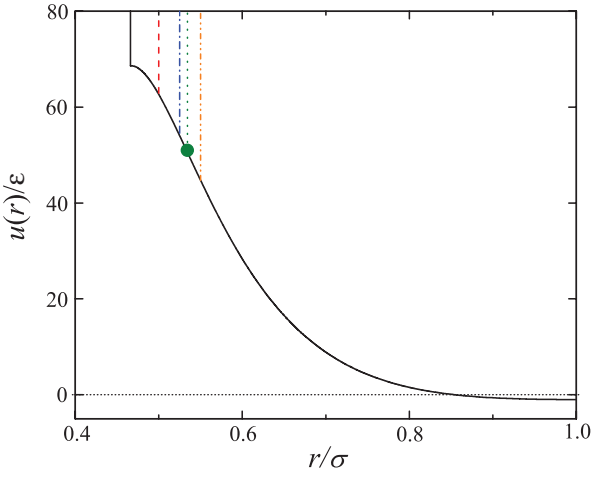

Figure 5. (Colour online). Modified exp-6 potential for $\alpha = 10$. The vertical lines correspond to different values of r_{cross} (see text for explanation): $0.4659 \approx \sigma_M$ (black solid line), 0.5 (red dashed line), 0.525 (blue dash-dotted line), $0.53442 \approx \sigma_F$ (green dotted line), 0.55 (orange double-dash dotted line). The full green dot marks the point, σ_F, where the second derivative of the potential vanishes.

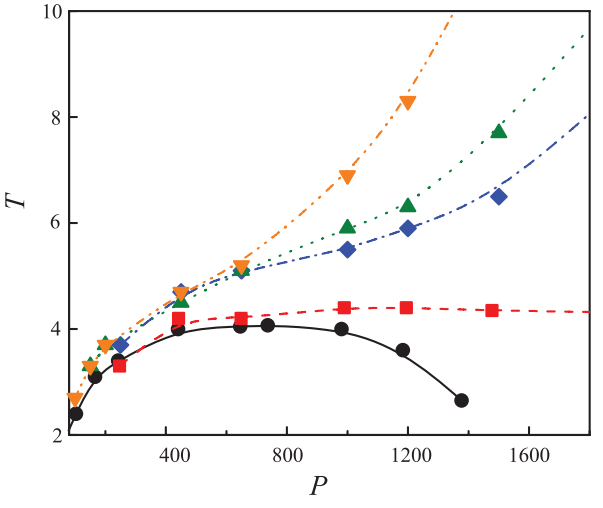

Figure 6. (Colour online). Phase diagram of the modified exp-6 potential for $\alpha = 10$ and for several values of r_{cross}: $0.4659 \approx \sigma_M$ (black solid line), 0.5 (red dashed line), 0.525 (blue dash-dotted line), $0.53442 \approx \sigma_F$ (green dotted line) and 0.55 (orange double-dash dotted line). The lines being shown are polynomial fits of the simulation data (full symbols).

high temperatures. As a result, the line of maximum density is swallowed up by the solid phase (in fact, for sufficiently large r_{cross}, the density maximum disappears completely). A similar behaviour has recently been observed for a family of isotropic pair potentials with two repulsive length scales [35]. The close relation between the occurrence of re-entrant melting and that of the density anomaly (be it in the stable or metastable fluid phase) points to a common origin for the two. Indeed, it appears that a prerequisite for both phenomena is the existence of two repulsive length scales, which in turn gives rise to two different patterns of local order in the system. Therefore, the crossover between low-density/low-temperature open structures and high-density/high-temperature compact ones is at the basis of the remelting of the solid into a denser fluid as well as of the decrease of the density upon isobaric cooling.

4. Conclusions

In this article, we have studied how the melting behaviour of a system of particles interacting through the exp-6 potential depends on the repulsion softness. We find that, by varying the softness parameter α, the anomalous features of the phase diagram do not change qualitatively while the typical pressure and temperature where re-entrant melting occurs change considerably. As the repulsion gets softer, i.e. as α decreases, the re-entrant-melting region moves to smaller pressures and temperatures. In fact, a softer repulsion and the associated length scale lose efficacy more rapidly with increasing pressure and temperature.

We have shown that the feature of the exp-6 potential that is crucial for the occurrence of anomalous melting is the existence of a concave region in the repulsive part of the potential. By progressively reducing the extent of this interval, in fact, the

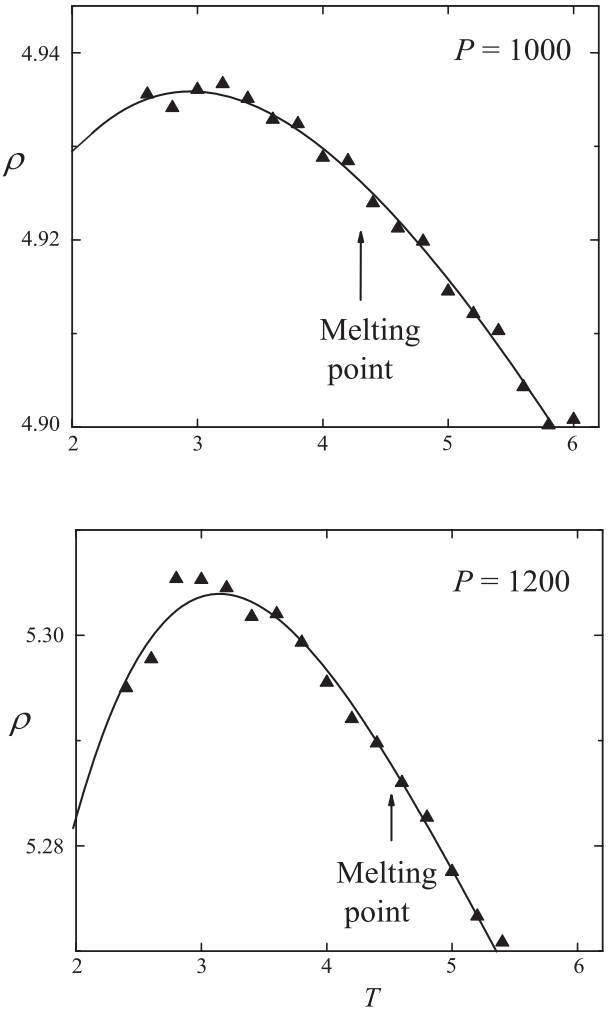

Figure 7. Modified exp-6 potential for $\alpha = 10$ and $r_{cross} = 0.5$: reduced number density of the fluid as a function of temperature for $P = 1000$ and 1200 (full triangles). All lines are fourth-order polynomial fits of the data points.

negatively-sloped portion of the melting line as well as the P–T region where the density is anomalous tend to disappear. This is an indication of the close relation between re-entrant melting and density anomaly, both phenomena being linked to the turning on and off of the two repulsive length scales in the system.

In spite of the modellistic nature of the system investigated, the sensitive dependence of the anomalous-melting region on the steepness of the repulsive interaction has a counterpart in real systems. By looking at the phase behaviour of elements displaying anomalous melting, it is possible to observe that the pressures and temperatures where the anomalies occur greatly vary from one element to the other. For example, the maximum in the melting line is at about 2 GPa for Cs [36], 30 GPa for Na [37] and is predicted around 100 GPa for H [38]. These experimental

and theoretical results can be rationalised by considering that atoms with more electrons are more susceptible, at least within the same chemical family, to pressure-induced structural softening. In addition to alkali metals, this trend is also observed for rare gases [39].

References

[1] D.A. Young, *Phase Diagrams of the Elements* (University of California Berkeley, 1991).
[2] H.J. Young and B.J. Alder, Phys. Rev. Lett. **38**, 1213; J. Chem. Phys. **70**, 473 (1979).
[3] P.F. McMillan, J. Mater. Chem. **14**, 1506 (2004).
[4] M. Ross and A.K. McMahan, Phys. Rev. B **21**, 1658 (1980).
[5] S. Prestipino, F. Saija, G. Malescio, Soft Matter, **5**, 2795 (2009).
[6] C.P. Royall, M.E. Leunissen, A.-P. Hynninen, and M. Dijkstra, J. Chem. Phys. **124**, 244706 (2006).
[7] C.N. Likos, Phys. Rev. **348**, 267 (2001).
[8] C.N. Likos, Soft Matter **2**, 478 (2006).
[9] G. Malescio, J. Phys.: Condens. Mat. **19**, 073101 (2007).
[10] Z. Yan, S.V. Buldryev, N. Giovambattista, and H.E. Stanley, Phys. Rev. Lett. **95**, 130604 (2005).
[11] A.B. De Oliveira, E.B. Neves, C. Gavazzoni, J.Z. Paukowski, P.A. Netz, and M.C. Barbosa, arXiv: 0904.1773.
[12] P.C. Hemmer and G. Stell, Phys. Rev. Lett. **24**, 1284 (1970).
[13] F.H. Stillinger, J. Chem. Phys. **65**, 3968 (1976).
[14] S. Prestipino, F. Saija, and P.V. Giaquinta, Phys. Rev. E **71**, 050102 (2005).
[15] A. Lang, C.N. Likos, M. Watzlawek, and H. Lowen, J. Phys.: Condens. Mat. **12**, 5087 (2000).
[16] D. Quigley and M.I.J. Probert, Phys. Rev. E **71**, 065701(R) (2005); *ibid*. **72**, 061202 (2005).
[17] H.M. Gibson and N.B. Wilding, Phys. Rev. E **73**, 061507 (2006).
[18] A.B. De Oliveira, P.A. Netz, and M.C. Barbosa, Eur. J. Phys. B **64**, 481 (2008).
[19] A.B. De Oliveira, M.C. Barbosa, and P.A. Netz, Physica A **386**, 744 (2007).
[20] P.G. De Benedetti, V.S. Raghavan, and S.S. Borick, J. Phys. Chem. **95**, 4540 (1991).
[21] R.A. Buckingham, Proc. R. Soc. London, Ser. A **168**, 264 (1938).
[22] L.E. Fried, W.M. Howard, P.C. Souers, Exp-6: a new equation of state library for high pressure thermochemistry, 12th International Detonation Symposium, August 11–16 (San Diego, USA, 2002).
[23] G. Malescio, F. Saija, and S. Prestipino, J. Chem. Phys. **129**, 241101 (2008).
[24] S.N. Luo, A. Strachan, and D.C. Swift, J. Chem. Phys. **120**, 11640 (2004).
[25] P.M. Chaikin and T.C. Lubensky, *Principles of Condensed Matter Physics* (Cambridge University Press, Cambridge, UK, 2000).
[26] F. Saija, S. Prestipino, and P.V. Giaquinta, J. Chem. Phys. **115**, 7586 (2001).
[27] F.A. Lindemann, Phys. Z. **11**, 609 (1910).
[28] J.J. Gilvarry, J. Chem. Phys. **102**, 308 (1956).
[29] E.J. Meijer and D. Frenkel, J. Chem. Phys. **94**, 1169 (1991).
[30] F. Saija, S. Prestipino, and P.V. Giaquinta, J. Chem. Phys. **124**, 244504 (2006).
[31] E.A. Jagla, J. Chem. Phys. **111**, 8980 (1999).
[32] M.R. Sadr-Lahijany, Phys. Rev. Lett. **81**, 4895 (1998).
[33] P. Kumar, S.V. Buldyrev, F. Sciortino, E. Zaccarelli, and H.E. Stanley, Phys. Rev. E **72**, 021501 (2005).
[34] Yu.D. Fomin, N.V. Gribova, V.N. Ryzhov, S.M. Stishov, and D. Frenkel, J. Chem. Phys. **129**, 064512 (2008).

[35] A.B. de Oliveira, P.A. Netz, and M.C. Barbosa, EPL **85**, 36001 (2009).
[36] A. Jayaraman, R.C. Newton, and J.M. McDonough, Phys. Rev. **159**, 527 (1967).
[37] E. Gregoryanz, O. Degtyareva, M. Somayazulu, R.J. Hemley, and H. Mao, Phys. Rev. Lett. **94**, 185502 (2005).
[38] S. A. Bonev, E. Schwegler, T. Ogitsu, and G. Galli, Nature **431**, 669 (2004).
[39] R. Boehler, M. Ross, P. Soderlind, and D. B. Boercker, Phys. Rev. Lett. **86**, 5731 (2005).